Solid State Phenomena
ISSN: 1662-9779, Vol. 359, pp 35-39
doi:10.4028/p-pSfz1z

Submitted: 2023-08-23
Revised: 2024-01-30
Accepted: 2024-02-04
Online: 2024-08-22

Dopant Activation Comparison in Phosphorus and Nitrogen Implanted 4H-Silicon Carbide

Suman Das[1,a*], Daniel J. Lichtenwalner[1,b], Hemant Dixit[1,c], Steven Rogers[1,d], Andreas Scholze[1,e], and Sei-Hyung Ryu[1,f]

[1]Wolfspeed, Inc., 4600 Silicon Drive, Durham, NC 27703, USA

[a]suman.das@wolfspeed.com, [b]daniel.lichtenwalner@wolfspeed.com, [c]hemant.dixit@wolfspeed.com, [d]steven.rogers@wolfspeed.com, [e]andreas.scholtze@wolfspeed.com, [f]sei-hyung.ryu@wolfspeed.com

Keywords: 4H silicon carbide (SiC), Hall measurement, activation, ionization, mobility.

Abstract. Bulk mobility and dopant activation of implanted species into 4H-SiC plays a crucial role in the carrier conduction, blocking behavior, and channel properties of a 4H-SiC vertical power MOSFET. Nitrogen and phosphorus ion implantation became the norm as n-type dopants for 4H-SiC. Therefore, the doping and temperature behavior of both species in 4H-SiC needs to be well characterized. In this study, we report a comparison in electrical characteristics between nitrogen and phosphorus implanted 4H-SiC as a function of temperature for various doping levels. For this purpose, 4-point van der Pauw samples are prepared, resistivity and Hall measurements are conducted. We found that resistivities drop as temperature increases from 140 K with phosphorus having higher resistivities at all implanted doping concentrations. The carrier concentrations increase with increase of temperature, indicating incomplete ionization of dopants. Mobilities drop at low temperature due to increased impurity scattering, reaches a peak near 300 K and drops at higher temperature due to increased phonon scattering. From the obtained data, using a two-level charge neutrality equation, the activation percentage and ionization energies of dopants in hexagonal and cubic sites for both species are extracted and compared.

Introduction

Silicon carbide is one of the major candidates as a wide band gap semiconductor for fabricating MOSFET power devices due to its native oxide being SiO_2, wide band gap, and ability to be doped both n and p-type [1]. In the improvement of current conduction of a 4H-SiC power MOSFET, both channel and bulk mobilities play an important role. Due to its low atomic mass and ease of implant activation in 4H-SiC, nitrogen (N) is a frequently utilized element for n-type doping. Nevertheless, because of phosphorus's (P) proximity to nitrogen in terms of ionization energies, it may also be employed as a substitute. Phosphorus's different atomic mass provides different implantation distribution (having a different projected range and straggle compared to nitrogen) [2], which may have benefit for device design. Despite nitrogen becoming a standard n-type dopant, a thorough investigation of both dopants is limited [3-7] in terms of doping concentrations and activation temperatures. A comparative research between N and P containing different doping concentrations would help to verify the activation percentage and ionization energies and will result in a greater comprehension of the characteristics of P and N as n-type dopants in 4H-SiC.

In this work, the bulk mobility is studied using nitrogen and phosphorus implantation into silicon carbide over a range of doping concentrations. After successful device fabrication, electrical characterization is performed to examine resistivity, carrier concentrations, and mobility. Examining all the parameters over a wide temperature range allows calculation of the activation percentage ratio, ionization energies of the dopants, and to examine any underlying benefits of using any specific dopant or a doping concentration. This information is key for building successful TCAD models for next generation device design, and performance optimization.

Experimental Methods

Circular van der Pauw structures were fabricated to study dopant electrical characteristics. N and P ions were implanted at room temperature using the same energies and doses to achieve uniform doping concentrations vs depth, ranging from about 4×10^{18} to 1.2×10^{19} cm^{-3}, on lightly doped n-type 4H-SiC epilayers (Si-face). Being a lighter element nitrogen penetrated deeper into 4H-SiC, yielding a 30% higher implant thickness and correspondingly lower average doping than phosphorus. A deeper P-well with a doping concentration of about $\sim2\times10^{17}$ cm^{-3} was formed for junction isolation, as shown in the inset of Fig. 1. All samples were activated under identical conditions, at a temperature above 1600 ºC. For ohmic contacts, Nickel was deposited using evaporation and post-annealed at high temperature. The structures were then mounted on 1cm x 1cm carrier boards. Typical current-voltage characteristics are shown in Fig. 1 for the phosphorus doped n-well samples, performed using 4-point probe resistance measurements at room temperature. The linear behavior of these curves indicates ohmic contacts. To determine carrier concentration and Hall mobility for various doping levels, Hall measurements were conducted. Ionization energy levels and dopant activation percentage are then computed using the two-level charge neutrality equation [3-8].

Results

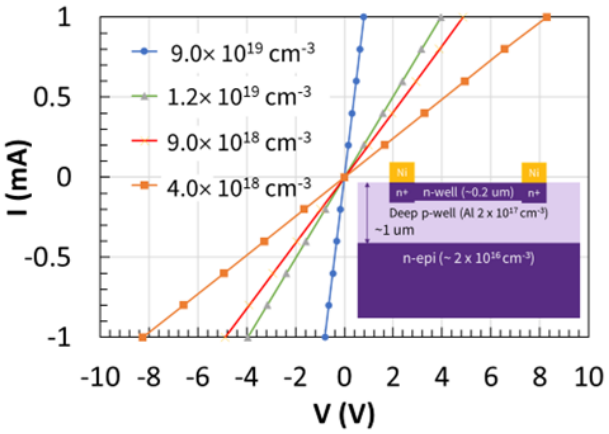

Fig. 1. Current-voltage measurements at 25°C for different P-doped n-well concentrations showing ohmic behavior of the contacts. Inset shows a schematic cross-sectional diagram of the van der Pauw structure.

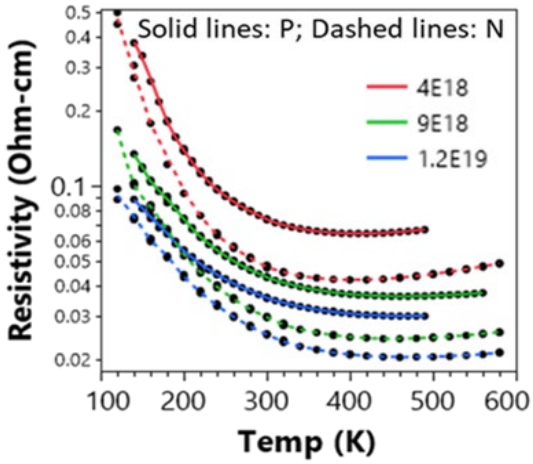

Fig. 2. Resistivity versus temperature for nitrogen and phosphorus for doping of 4×10^{18}, 9×10^{18}, and 1.2×10^{19} cm^{-3}.

Figure 2 shows a comparison of the resistivity as a function of temperature for N versus P at identical implant doses. Nitrogen (dashed lines) shows a lower value of resistivity compared to phosphorus in these doping levels. Resistivity for both dopants drops as temperature increases in the range from 150 to 300 K, while above room temperature, a small increase in resistivity can be observed. The resistivity behavior for these implanted samples is similar to the in situ doped substrates as reported earlier [9].

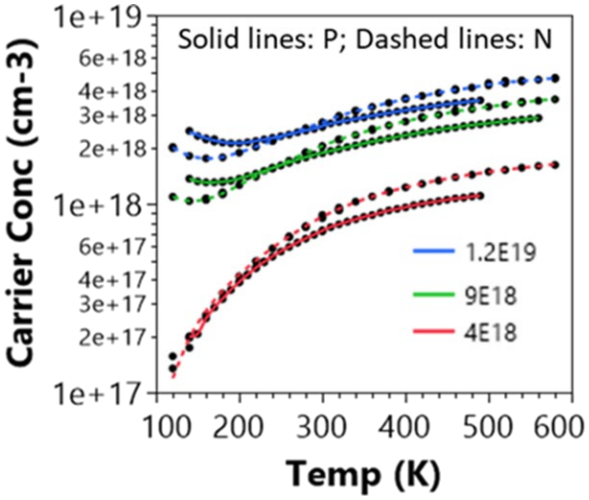

Fig. 3. Carrier concentration versus temperature for nitrogen and phosphorus with doping concentration of 4×10^{18}, 9×10^{18}, 1.2×10^{19} cm^{-3} versus temperature from Hall measurement, revealing incomplete ionization.

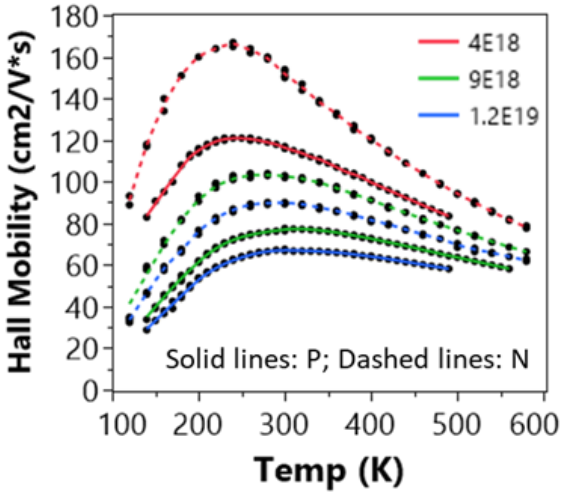

Fig. 4. Hall mobility versus temperature for nitrogen and phosphorus with doping of 4×10^{18}, 9×10^{18}, 1.2×10^{19} cm^{-3}, revealing impurity scattering at low temperature and phonon scattering at high temperature.

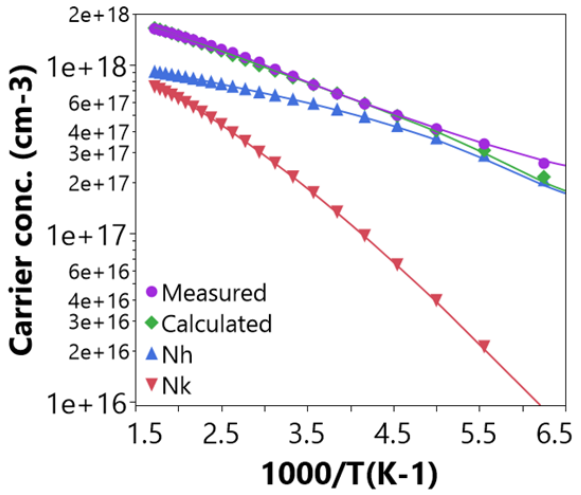

Fig. 4. Typical plot showing the extracted hexagonal carrier concentration and cubic dopant concentrations vs temperature for nitrogen doping of 4×10^{18} cm^{-3}.

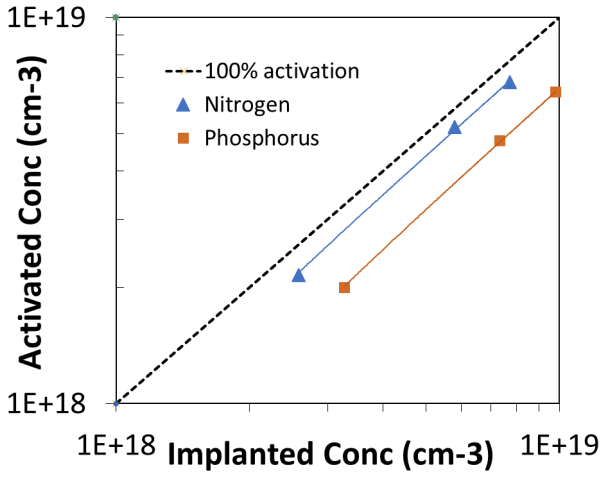

Fig. 5. Activated doping concentration versus implanted doping concentration for N and P. N shows around 90% activation, while P shows a lower activation percentage ~ 60%.

species (nitrogen and phosphorus) of dopants, and reaches a saturation level at high temperature, which proves incomplete ionization at lower temperature. Above 300 K, nitrogen shows higher Hall measurements are conducted that show the presence of incomplete ionization at lower temperature. Figure 3 shows that the carrier concentration increases with temperature for both carrier concentration (n_s) compared to phosphorus. A minor increase in n_s at very low temperature (150 K) occurs possibly due to the impacts of the p-well dopant freeze out or a change in effective implant thickness with temperature. This characteristic of the data requires further study. Figure 4 shows a mobility comparison at different temperatures. Here for these doping levels, N produces a higher mobility as compared to P. The difference in mobility becomes more prominent at low doping concentrations. For both the dopants, mobility drops at lower temperatures due to increased ionized impurity scattering. It reaches a peak value near 300 K and falls as temperature increases due to increased phonon scattering.

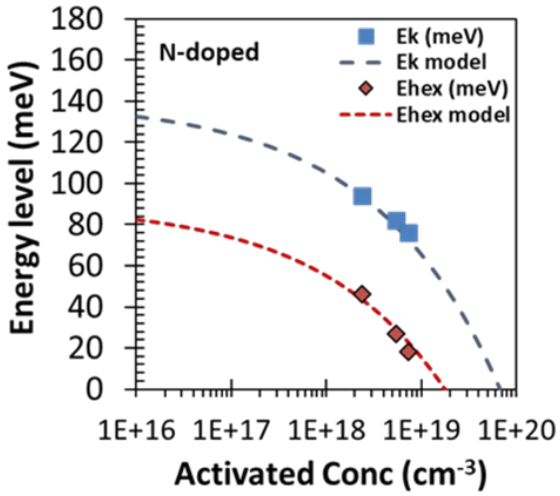

Fig. 7. Ionization energies for nitrogen implanted samples for different doping concentrations. Hexagonal site energy is practically 0 meV by 2×10^{19} cm^{-3} doping.

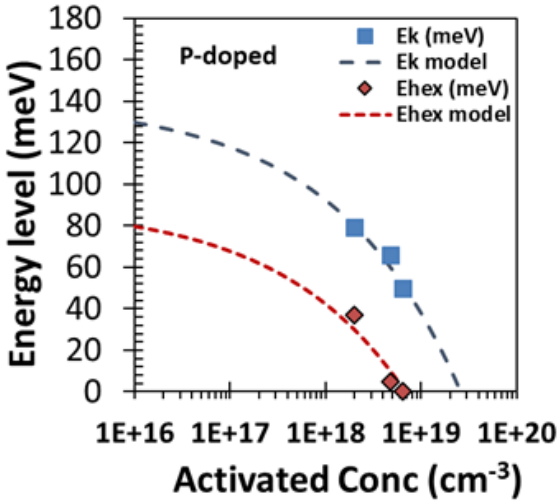

Fig. 8. Ionization energies for phosphorus implanted samples for different doping concentration. Hexagonal site energy is practically 0 meV by 1×10^{19} cm^{-3} doping.

The carrier concentration (n_s) information is used in a two-level charge neutrality equation to calculate activated doping percentage and ionization energies related to specific dopants. Figure 5 shows a measured n_s versus 1000/T curve, modeled with a predicted activated concentration and assigned specific ionization energies to hexagonal and cubic lattice sites (50:50) [3-6]. The values of the ionization energies for hexagonal and cubic sites as a function of doping concentration follow the two-level charge neutrality model [3-8]. The percentages of activated dopants calculated here from this analysis are plotted as a function of doping concentrations as shown in Fig. 6. Nitrogen activates near 90% for all the doping levels, whereas phosphorus activates around 60%, and activation rates seem to drop slightly at higher implanted concentration. Figure 7 and Fig. 8 show extracted ionizations energies for nitrogen and phosphorus, respectively. For both dopants, the extracted values follow the Pearson-Bardeen model denoted by dotted lines. The ionization energies for the hexagonal sites goes to zero for nitrogen and phosphorus near $2x10^{19}$ cm^{-3} and $1x10^{19}$ cm^{-3} respectively.

Comparing phosphorus to nitrogen-implanted samples, with similar doping levels and activation temperatures, phosphorus exhibits slightly lower ionization energies for hexagonal and cubic sites, in comparison with nitrogen. The ionization energies calculated here are generally in agreement with earlier studies and theoretical models [3-6]. Based on the analysis, phosphorus appears to be a suitable n-type dopant. To properly quantify implantation damage with phosphorus, more investigation is necessary. Given that phosphorus has a larger mass than nitrogen, which influences both the implantation depth and the distribution of doping, more research is required in this area.

Conclusion

Electrical characteristics of nitrogen and phosphorus implanted 4H-SiC is compared by four-point probe resistivity and Hall measurements. Nitrogen is observed to have lower resistivities in the measured temperature range for all doping levels used in this study. Carrier concentrations versus temperature indicates incomplete ionization at low temperatures with nitrogen having higher carrier concentrations at higher temperatures. Mobility comparison for two species yields higher mobility for nitrogen, along with a lower resistivity at all temperatures. Mobilities for all doping concentrations reduces at temperatures below 300 K due to an increase in impurity scattering and drops above room temperatures due to increased phonon scattering. Activation percentages and ionization energies are extracted using two level charge neutrality equation. Nitrogen implanted 4H-SiC shows a ~90% dopant activation whereas phosphorus shows a ~60% activation of dopants. Ionization energies for nitrogen and phosphorus follows theoretical trends.

The thorough analysis of activation percentages and ionization energies will be useful for successful calibration of device modeling and simulations of 4H-SiC based devices.

References

[1] T. Kimoto, J.A. Cooper, Fundamentals of Silicon Carbide Technology (John Wiley & Sons, Singapore 2014).

[2] M.S. Janson; M. K. Linnarsson; A. Hallén; B. G. Svensson, J. Appl. Phys. 93, 8903–8909 (2003)

[3] M.A. Capano, J.A. Cooper, Jr., M.R. Melloch, A. Saxler and W.C. Mitchel, J. Appl. Phys. 87, 8773 (2000).

[4] J. Pernot, W. Zawadzki, S. Contreras, J. L. Robert, E. Neyret, and L. Di Cioccio, J. Appl. Phys 90, 1869 (2001).

[5] W. Gotz, A. Schoner, and G. Pens1, W. Suttrop and W. J. Choyke, R. Stein and S. Leibenzeder; Applied Physics 73, 3332 (1993);

[6] M. Laube, F. Schmid, G. Pensl, and G. Wagner, Materials Science Forum, 389-393, 791 (2002)

[7] J. Pernot, S. Contreras and J. Camassel, Journal of Applied Physics 126, 145701 (2019);

[8] F. Schmid and G. Pensl, Appl. Phys. Lett. 84, 3064 (2004)

[9] D.J. Lichtenwalner, J.H., Park, S. Rogers, H. Dixit, A. Scholtze, S. Bubel, and S.H. Ryu, Materials Science Forum, 1089, 3–7 (2023).